Chemical Science

Accepted Manuscript

This article can be cited before page numbers have been issued, to do this please use: H. Wu, J. Song, H. Liu, Z. Xie, C. Xie, Y. Hu, X. Huang, M. Hua and B. Han, *Chem. Sci.*, 2019, DOI: 10.1039/C9SC00322C.

ROYAL SOCIETY OF CHEMISTRY

rsc.li/chemical-science

ROYAL SOCIETY OF CHEMISTRY
View Article Online
DOI: 10.1039/C9SC00322C

Journal Name

ARTICLE

Electrocatalytic route for transformation of biomass-derived furfural to 5-hydroxy-2(5H)-furanone

Received 00th January 20xx,
Accepted 00th January 20xx

DOI: 10.1039/x0xx00000x

www.rsc.org/

Haoran Wu,[a,b] Jinliang Song,*[a] Huizhen Liu,[a,b] Zhenbing Xie,[a,b] Chao Xie,[a,b] Yue Hu,[a,b] Xin Huang,[a,b] Manli Hua,[a,b] and Buxing Han*[a,b]

Development of efficient strategies for biomass valorization is a highly attractive topic. Herein, we conducted the first work for electrocatalytic oxidation of renewable furfural to produce the key bioactive intermediate 5-hydroxy-2(5H)-furanone (HFO). It was demonstrated that using H_2O as the oxygen source and metal chalcogenides (CuS, ZnS, PbS, *etc*.) as electrocatalysts, the reaction could proceed efficiently, and the CuS nanosheets prepared in this work showed the best performance to provide high selectivity (83.6%) of HFO and high conversion (70.2%) of furfural. Meanwhile, the CuS electrocatalyst showed a long-term stability. Mechanism investigation showed that furfural was oxidized to HFO *via* multistep reactions, including C-C cleavage, subsequent ring-opening and oxidation, and intramolecular isomerization.

Introduction

With the gradual depletion of fossil resources, utilization of renewable and abundant biomass to produce valuable chemicals and functional materials has become a very interesting field.[1-5] In this regard, producing valuable chemicals using lignocellulose-derived furfural has attracted much attention.[6-8]

5-Hydroxy-2(5H)-furanone (HFO) is a key constituent in many biologically active compounds or intermediates.[9] HFO could be synthesized by thermo-catalytic oxidation of high-cost 2-trialkylsilyloxyfurans with dimethyldioxirane as oxidant.[10] In comparison, direct oxidation of the renewable furfural to produce high value-added HFO *via* thermo-oxidation is highly desired. However, it was very difficult to obtain HFO selectively from direct thermo-oxidation of furfural because HFO was easily transformed to maleic acid (MA) under the thermocatalytic conditions.[11] In current reports about furfural thermo-oxidation,[12] HFO was only considered as the intermediate to synthesize MA, and no successful work has been reported with HFO as the target product from direct thermo-oxidation of furfural. On the other hand, photocatalysis has been applied in the oxidation of furfural or its derivatives (*i.e.*, furfuryl alcohol and furoic acid) to prepare HFO.[13-15] Although progress has been made in photo-oxidation of furfural to HFO, the reliance on environmentally hazardous photosensitizers and their poor recyclability severely limited the applications of the photocatalytic processes. Therefore, development of green, selective, and efficient routes for direct oxidation of furfural to HFO is highly desired but is challenging.

Recently, electrocatalysis has sparked increasing interest due to its potential ability of solving thermodynamic and/or kinetic problems in thermocatalysis and photocatalysis. The pathway of electrocatalytic reaction is often different from those of thermocatalysis and photocatalysis. Electrocatalysis has been widely applied in the fields of hydrogen and oxygen evolution, CO_2 conversion, and biomass transformation.[16-21] Moreover, some active species (*e.g.*, hydroxyl radicals) for oxidation (especially in water treatment for waste oxidation) can be generated from H_2O *via* electrocatalysis.[22-27] Considering the advantages of electrocatalysis, it may be a promising route for direct oxidation of furfural to HFO using H_2O as the oxygen source, but this has not been reported up to date.

In this work, we proposed the electrocatalytic route for the oxidation of furfural to HFO and formic acid (Scheme 1). By employing simple metal chalcogenides (*i.e.*, CuS, ZnS, PbS, *etc.*) as the electrocatalysts, furfural could be selectively oxidized into HFO using H_2O as the oxygen source at ambient conditions in a ternary electrolyte consisting of triethylammonium nitrate ($[Et_3NH]NO_3$), acetonitrile (MeCN) and H_2O, and the synthesized CuS nanosheets provided the best performance with a high selectivity (83.6%) of HFO and high conversion (70.2%) of furfural. To the best of our knowledge, this is the first work to realize the oxidation of furfural to HFO *via* electrocatalysis.

[a] Beijing National Laboratory for Molecular Science, CAS Key Laboratory of Colloid and Interface and Thermodynamics, CAS Research/Education Center for Excellence in Molecular Sciences, Institute of Chemistry, Chinese Academy of Sciences, Beijing 100190, China. E-mails: songjl@iccas.ac.cn; hanbx@iccas.ac.cn.
[b] School of Chemistry and Chemical Engineering, University of Chinese Academy of Sciences, Beijing 100049, China.

† Footnotes relating to the title and/or authors should appear here.
Electronic Supplementary Information (ESI) available: [details of any supplementary information available should be included here]. See DOI: 10.1039/x0xx00000x

View Article Online DOI: 10.1039/C9SC00523C

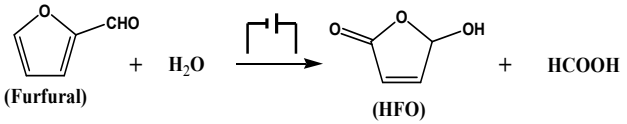

Scheme 1. Electrocatalytic oxidation of furfural to HFO.

Results and discussion

Synthesis and characterization of electrocatalysts

Metal chalcogenides (*e.g.*, MoS_2, Cu_2S, ZnS, CdS) have been considered as simple and efficient electrocatalysts owing to their unique electrical properties.[28-30] Therefore, metal chalcogenides can be potentially applied as the promising electrode materials for electro-oxidation. Initially, the CuS was synthesized *via* a solvothermal process in a deep eutectic solvent consisting of PEG-200 and thiourea, and the detailed preparation procedure is described in Experimental Section. X-ray diffraction (XRD) examination was conducted to confirm the formation of CuS. The pattern in Fig. 1A showed the characteristic peaks of CuS (JCPDS: 65-3588), verifying that CuS could be indeed generated by the proposed route. Meanwhile, X-ray photoelectron spectra (XPS) showed the characteristic binding energy of Cu^{2+} (Cu $2p_{3/2}$ 931.7 and Cu $2p_{1/2}$ 951.6 eV) and S^{2+} (S $2p_{3/2}$ 161.6 and S $2p_{1/2}$ 162.7 eV) in the prepared material (Figs. 1B and S1), further indicating the formation of CuS.[31] Furthermore, as clearly shown in scanning electron microscopy (SEM, Fig. 1C) and transmission electron microscopy (TEM, Fig. 1D) images, the prepared CuS had a nanosheet structure. For comparison, ZnS and PbS were also synthesized using the similar route with that for CuS preparation, and were characterized in detail by employing XRD, XPS, SEM and TEM (Figs. S2 and S3).

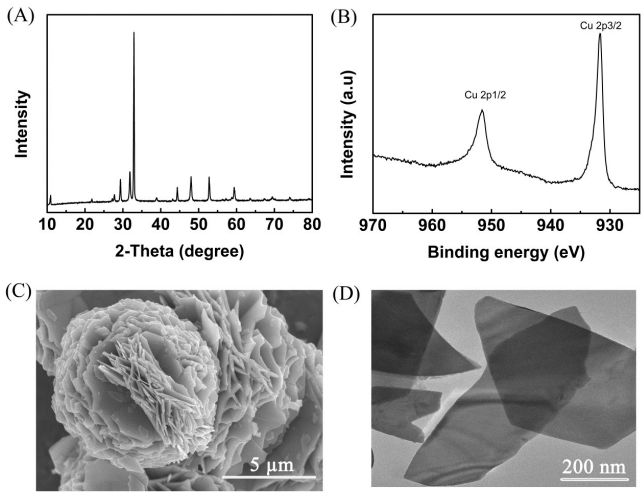

Fig. 1. Characterization of the prepared CuS. (A) XRD pattern, (B) XPS of Cu 2p, (C) SEM image, and (D) TEM image.

Performance of various electrocatalysts

The obtained metal chalcogenides (MC) were spread onto carbon paper (CP) as the electrodes (denoted as MC/CP) for the electrochemical oxidation of furfural. The electrocatalytic performance of the prepared MC/CP electrodes was initially evaluated by linear sweep voltammetry (LSV) measurements, which were conducted in an H-type cell containing three electrodes.[32] In the experiments, a ternary electrolyte consisting of $[Et_3NH]NO_3$, MeCN and H_2O was used as the anolyte, while aqueous H_2SO_4 solution (0.2 M) was employed as the catholyte. Meanwhile, the applied potential was swept from 0.3 to 1.9 V *vs.* Ag/Ag^+ with a scan rate of 20 $mV{\cdot}s^{-1}$. An obvious increase in current density could be found in the reaction systems with furfural in comparison to those without furfural (Figs. 2, S4-S8), suggesting the occurrence of furfural electro-oxidation on the prepared MC/CP electrodes.

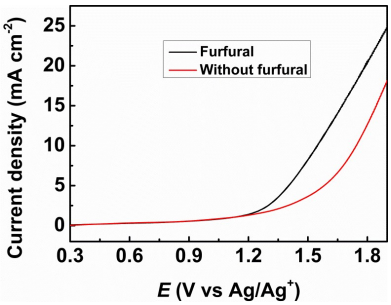

Fig. 2. LSV measurements using CuS/CP electrode for the electrochemical oxidation of furfural in $[Et_3NH]NO_3$ (1.8 wt%)-MeCN-H_2O (12.5 wt%) electrolyte.

The performance of various prepared electrodes for the electrochemical oxidation of furfural was subsequently examined (Table 1). In the reaction process, the main liquid products were HFO, maleic acid (MA), and HCOOH along with very small amount of maleic anhydride and 2(5H)-furanone (Scheme S1). As shown in Scheme 1, HCOOH could be generated and the selectivity was above 95% in all experiments. Meanwhile the gaseous product was O_2 from water electrolysis. As shown in Table 1, the prepared CuS/CP electrode (Table 1, entry 1) showed the best performance compared with ZnS/CP, PbS/CP, CdS/CP, MoS_2/CP, and WS_2/CP (Table 1, entries 2-6). As a comparison, copper oxide (CuO) was also employed as an electrocatalyst. Unfortunately, the CuO/CP electrode showed poorer electrocatalytic performance (Table 1, entry 7) than the prepared CuS/CP electrode (Table 1, entry 1).Moreover, the synthesized CuS nanosheets showed higher activity than commercial CuS of irregular particles (Fig. S9). N_2 adsorption-desorption isotherms (Fig. S10) showed that no micropores existed in both prepared CuS and the commercial one,[33,34] and they had same average pore diameter (3.82 nm). Meanwhile, the prepared CuS (18.0 $m^2\ g^{-1}$) showed a higher BET surface area than the commercial one (12.7 $m^2\ g^{-1}$). The higher surface area and the nanosheet structure of the synthesized CuS were helpful for the exposure of more active sites,[35] and thus the activity of synthesized CuS was higher than the commercial one. Additionally, when using bare carbon paper as the electrode (Table 1, entry 9), the furfural conversion and FE were much lower than those over the synthesized CuS/CP (Table 1, entry 1), implying the catalytic role of the CuS for furfural oxidation.

Electrochemical impedance spectroscopy (EIS) was carried out to get more interfacial information of

View Article Online
DOI: 10.1039/C9SC00328C

electrode/electrolyte (Figs. S11-17 and Table S1), and a simple equivalent circuit was used to fit the high and medium frequency data (Fig. S18). As shown in Table S1, CuS/CP showed the lowest charge transfer resistances (R_{ct}, 34.51) among the determined electrodes (*i.e.*, CuS/CP, ZnS/CP, PbS/CP, CdS/CP, MoS_2/CP, WS_2/CP, and CuO/CP), indicating more facile electron transfer between the interface of CuS/CP and the anolyte. Meanwhile, the highest double layer capacitance (C_{dl}) was achieved using the CuS/CP electrode (Table S1), suggesting the higher charge density around CuS/CP. Both more facile electron transfer and higher charge density were beneficial for the generation of hydroxyl radicals (the active species for oxidation) from H_2O electrolysis,[22-27] and thus enhanced the furfural oxidation on the CuS/CP electrode. Additionally, no obvious difference was found for solution resistance (R_s) because the electrolyte with same compositions was employed for all reactions (Table 1), implying the negligible effect of R_s on the different activity of the used electrodes. The results above suggested that the prepared CuS/CP was a superior electrode for the electrochemical oxidation of furfural to generate HFO owing to its lowest R_{ct} and highest C_{dl}.

Table 1. Electrochemical oxidation of furfural on different electrodes at an applied potential of 1.6 V (*vs.* Ag/Ag$^+$) in the $[Et_3NH]NO_3$ (1.8 wt%)-MeCN-H_2O (12.5 wt%) electrolyte (5.6 g) with 1 mmol of furfural for 7 h electrolysis.

Entry	Electrode	Conversion (%)[a]	Selectivity (%)[a]		FE (%)[b]
			HFO	MA	
1	CuS/CP	70.2	83.6	8.8	77.1
2	ZnS/CP	56.3	89.9	8.1	76.9
3	PbS/CP	63.7	83.5	9.4	78.3
4	CdS/CP	51.7	65.4	6.5	64.9
5	WS_2/CP	69.9	68.7	9.4	69.2
6	MoS_2/CP	61.4	64.2	6.9	63.4
7	CuO/CP	55.1	71.5	13.7	78.9
8[c]	CuS/CP	53.5	85.5	9.3	75.2
9	CP	23.8	72.3	10.1	61.8

[a]The conversion and selectivity were obtained from NMR examinations. [b]FE represented the sum of faradaic efficiency of HFO and MA in this work. [c]Commercial CuS was used as the electrocatalyst.

Effect of various reaction parameters

The effect of applied potential on the electrochemical oxidation of furfural in $[Et_3NH]NO_3$ (1.8 wt%)-MeCN-H_2O (12.5 wt%) electrolyte was investigated. As shown in Fig. 3A, at a lower applied potential (1.5 V *vs.* Ag/Ag$^+$), the selectivity of HFO could reach 89.6%, but the furfural conversion was low (54.6%). With the increase of the applied potential, the conversion of furfural gradually increased, while the selectivity of HFO gradually decreased with the increasing MA selectivity. The results indicated that lower applied potential was not beneficial for furfural conversion because less amount of hydroxyl radicals were generated at lower applied potential, and higher potential resulted in forming more hydroxyl radicals, which enhanced conversion of HFO to MA. Control experiments using HFO as the reactant proved that the conversion of HFO increased with the increasing applied potential over the prepared CuS/CP electrode (Fig. S19). In addition, higher potential caused more oxygen evolution (a competitive reaction),[36] resulting in the decrease of the faradaic efficiency. Therefore, 1.6 V (*vs.* Ag/Ag$^+$) was selected as the optimal potential for the following investigation.

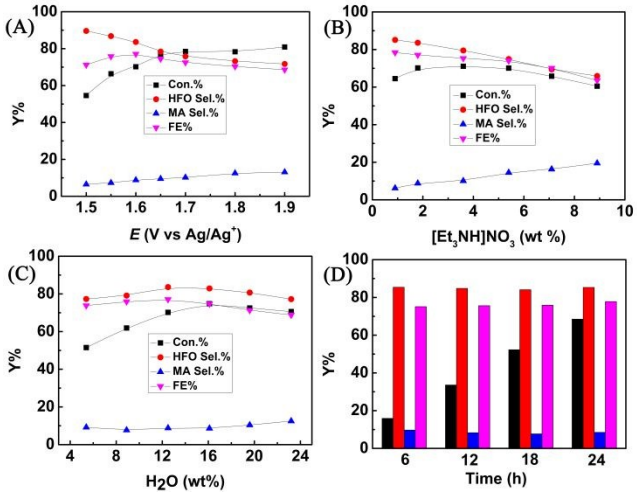

Fig. 3. Effects of various parameters on electrochemical oxidation of furfural to HFO over CuS/CP electrode in $[Et_3NH]NO_3$-MeCN-H_2O electrolyte (5.6 g) with 1 mmol of furfural for 7 h. (A) Applied potential, (B) $[Et_3NH]NO_3$ concentration, (C) H_2O concentration, and (D) long time electrolysis for furfural oxidation using CuS/CP electrode in $[Et_3NH]NO_3$ (1.8 wt%)-MeCN-H_2O (12.5 wt%) electrolyte (7.6 g) with 3 mmol of furfural at 1.6 V *vs.* Ag/Ag$^+$. (Black, red, blue, and magenta bars represented furfural conversion, HFO selectivity, MA selectivity, and FE, respectively.)

The composition of the anolyte could also significantly affect the electrochemical oxidation of furfural. In one aspect, the effect of $[Et_3NH]NO_3$ concentration was evaluated (Fig. 3B). Higher concentration of $[Et_3NH]NO_3$ could result in higher conductivity (Table S2), which was beneficial for the generation of hydroxyl radicals. More hydroxyl radicals would enhance further oxidation of HFO to MA, and thus the selectivity of HFO decreased with the increasing of $[Et_3NH]NO_3$ concentration. Meanwhile, the FE and the furfural conversion also decreased at higher $[Et_3NH]NO_3$ concentration because higher conductivity was also prone to enhance the oxygen evolution (a competitive reaction).[36] Additionally, lower concentration (0.9 wt%) of $[Et_3NH]NO_3$ was not beneficial for furfural conversion because lower conductivity was unhelpful for the formation of hydroxyl radicals. Therefore, by balancing the conversion and selectivity, 1.8 wt% of $[Et_3NH]NO_3$ was the optimal concentration. In another aspect, H_2O was indispensable for electrochemical oxidation because it could provide hydroxyl radicals as the active species for the oxidation.[22-27] Therefore, the effect of H_2O concentration in anolyte was examined (Fig. 3C). The conversion of furfural increased with increasing H_2O amount within a certain concentration range (5.4-16.1 wt%) because H_2O was helpful

for the dissociation of ion pairs in $[Et_3NH]NO_3$ to enhance the generation of hydroxyl radicals, but the selectivity of HFO reached the maximum at 12.5 wt% of H_2O. However, higher concentration of H_2O (> 12.5 wt%) was not beneficial for furfural oxidation to generate HFO because too much H_2O provided more hydroxyl radicals, and thus enhanced the competitive oxygen evolution and further oxidation of HFO, resulting in a decrease in the selectivity of HFO and FE. Therefore, 12.5 wt% of H_2O was the suitable concentration in our electrocatalytic system. Finally, the long-term persistence of the prepared CuS/CP electrode was examined (Fig. 3D). High selectivity (85.3%) of HFO and high FE (77.8%) could be achieved with a reaction time of 24 h. Meanwhile, no obvious changes were found in the XRD patterns (Fig. S20) and XPS spectra of Cu 2p and S 2p (Fig. S21) of the virgin and used CuS/CP electrode, suggesting no other species was formed and no oxidation of CuS surface was occurred after electrocatalysis (24 h). The results above suggested the excellent long-term stability of the prepared CuS/CP electrode.

Furthermore, furfural concentration was also an important parameter to affect the reaction efficiency. Herein, the influence of furfural concentration on the electro-oxidation was investigated. As shown in Fig. 4, the furfural conversion gradually decreased with the increasing of furfural concentration. It was known that the amount of the formed hydroxyl radicals was certain with the certain reaction time and applied potential, which caused that the amount of furfural converted was certain, and thus the conversion decreased with the increasing of furfural concentration. In contrast, no obvious difference was found for the product (HFO and MA) selectivities and the FE. These results indicated that furfural concentration affected its conversion rather than the product selectivities and the FE at a certain reaction time and applied potential.

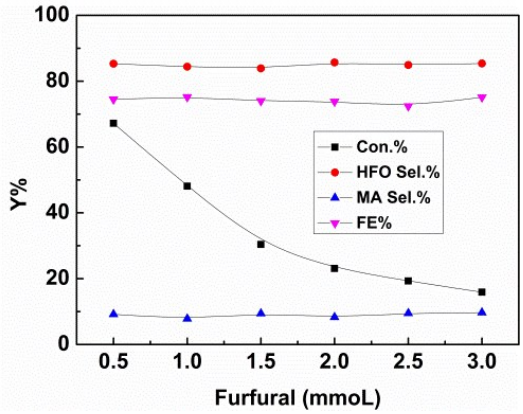

Fig. 4. Effect of furfural concentration on the electrochemical oxidation of furfural over CuS/CP electrode in the electrolyte (7.6 g) of $[Et_3NH]NO_3$ (1.8 wt%)-MeCN-H_2O (12.5 wt%) for 6 h.

Reaction mechanism

To better understand the reaction mechanism for furfural electro-oxidation to HFO, several control experiments were conducted under the above optimal reaction conditions. First, furoic acid was used as the reactant considering that furfural could be easily oxidized to furoic acid. However, the selectivity of HFO was only 48.1% from the electro-oxidation of furoic acid (Scheme 2A) along with a very low selectivity of HCOOH (3.3%) while the selectivity of HCOOH was above 95% using furfural as the reactant. These results indicated that furoic acid was not the main intermediate in the electrochemical oxidation of furfural to HFO. Second, no furan was generated in the process of furfural electro-oxidation, and control experiment also showed that no HFO was formed when using furan as the reactant, suggesting that the formation of furan *via* the cleavage of the C-C bond (Scheme 2B) was not the reaction pathway. Third, in order to better obtain the reaction intermediates, 5-methylfurfural with the similar structure to furfural was used as the reactant (Scheme 3). Through ^1H NMR and GC-MS analysis, HCOOH, 5-methyl-2(3H)-furanone (intermediate 2), intermediate 3, and 3-acetylacrylic acid were detected in the electrochemical oxidation of 5-methylfurfural (Fig. S22). The results above indicated that 5-methyl-2(3H)-furanone (intermediate 2) was formed *via* the cleavage of the C-C bond to generate HCOOH and subsequent isomerization with the aid of the hydroxyl radicals generated by electrocatalysis. In one pathway (Path I in Scheme 3), the generated 5-methyl-2(3H)-furanone could be converted to intermediate 3. Then, intermediate 3 could be further oxidized to 3-acetylacrylic acid. In another potential pathway (Path II in Scheme 3), 5-methyl-2(3H)-furanone could be transformed into levulinic acid (not detected) *via* hydrolysis, and levulinic acid was not able to be oxidized to 3-acetylacrylic acid in a control experiment using levulinic acid as the reactant. The results above suggested that 5-methyl-2(3H)-furanone was transformed through the reaction pathway of Path I (Scheme 3). Based on above discussion, we could speculate that furfural could be converted into HFO by the similar route with Path I.

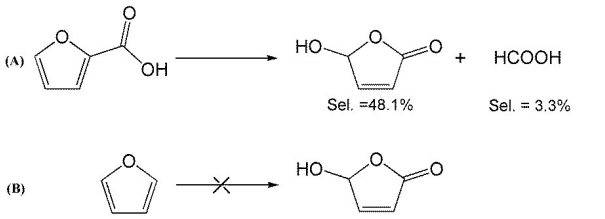

Scheme 2. Control experiment using furoic acid and furan as the reactant.

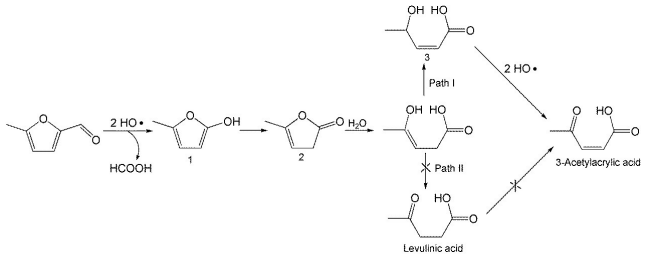

Scheme 3. Control experiment using 5-methylfurfural as the reactant.

On the basis of the results obtained in this work and some reported knowledge,[11,22-27] a reasonable mechanism was proposed for the electrochemical oxidation of furfural to HFO (Scheme 4). Initially, the hydroxyl radicals[22-27] were generated from H_2O by losing electron on the surface of CuS/CP electrode. Then, intermediate 4 and HCOOH were generated *via* the cleavage of C-C of furfural with the aid of the generated hydroxyl radicals, and the formed intermediate 4 was quickly converted into intermediate 5 *via* rearrangement. After the above steps, intermediate 6 (Fig. S23) was formed through a pathway like the Path I (Scheme 3) using 5-methylfurfural as the reactant. Finally, HFO was generated through the isomerization of intermediate 6.[11] In addition, HFO could be partially oxidized to MA by the formed hydroxyl radicals in the reaction process.

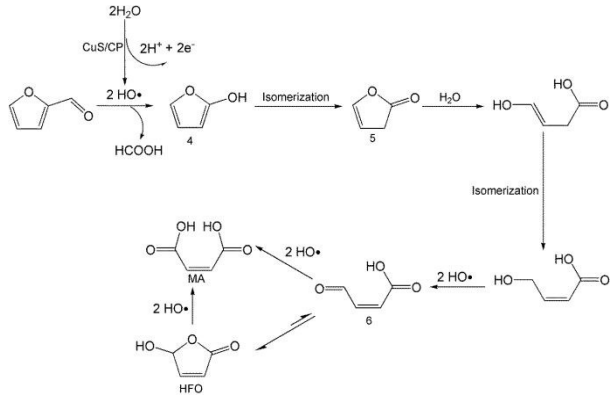

Scheme 4. Possible reaction mechanism for electrochemical oxidation of furfural to HFO over CuS/CP electrode in $[Et_3NH]NO_3$-MeCN-H_2O anolyte.

Conclusions

In conclusion, electrochemical oxidation of furfural to HFO was realized for the first time by employing metal chalcogenides (*i.e.*, CuS, ZnS, PbS, CdS, WS_2, and MoS_2) as the electrocatalysts and H_2O as the oxygen source at ambient conditions. Among the used electrodes, the CuS/CP prepared in this work showed the best performance, and high selectivity (83.6%) of HFO could be obtained with a furfural conversion of 70.2% in a ternary anolyte consisting of $[Et_3NH]NO_3$ (1.8 wt%), MeCN, and H_2O (12.5 wt%). Moreover, the prepared CuS/CP electrode showed excellent long-term persistence for the electrochemical oxidation of furfural to HFO. Mechanism investigation indicated that HFO was generated through multistep reactions, including the cleavage of C-C bond, subsequent ring-opening and oxidation, and intramolecular isomerization. This work opens the avenue to produce high value-added HFO *via* electrochemical oxidation of renewable furfural using H_2O as the oxygen source. We believe that the electrocatalytic strategy can also be used to explore the routes for efficient transformation of other furan derivatives to valuable chemicals.

Experimental

View Article Online
DOI: 10.1039/C9SC00322C

Materials

Triethylammonium nitrate ($[Et_3NH]NO_3$, 98%) was purchased from the Centre of Green Chemistry and Catalysis, Lanzhou Institute of Chemical Physics, Chinese Academy of Sciences. Polyethylene glycol (PEG-200, 99%), thiourea (99%), molybdenum disulfide (99%), and copper oxide (CuO, 97%) were supplied by J&K Scientific Co., Ltd. Tungsten sulphide (99%) was purchased from Adamas Reagent Co., Ltd. Copper nitrate trihydrate (99%), lead acetate trihydrate (99%) and zinc nitrate hexahydrate (99%) were obtained from Sinophar Chemical Reagent Co., Ltd. Nafion D-521 dispersion (5% w/w in water and 1-propanol, ≥0.92 meg/g exchange capacity), Nafion N-117 membrane (0.180 mm thick, ≥0.90 meg/g exchange capacity), copper sulfide (99.8%), cadmium sulphide (98%) and Toray Carbon Paper (CP, TGP-H-60, 19×19 cm) were purchased from Alfa Aesar China Co., Ltd.

Preparation of metal chalcogenides (MC)

The procedures were discussed taking the preparation of CuS as an example. First, a deep eutectic solvent consisting of thiourea and PEG-200 with the mole ratio of 1:2 was prepared on the basis of the reported method.[37] Then, $Cu(NO_3)_2{\cdot}3H_2O$ (1.0 g) was dissolved into the prepared deep eutectic solvent (40.0 g) under stirring. After that, the mixture was transferred into a stainless steel reactor with a Teflon coating, and the reactor was maintained at 180 °C for 24 h. Finally, the prepared CuS was washed by ethanol and water for three times, and was dried under vacuum at 40 °C for 24 h. The preparation process of PbS and ZnS was similar with that for preparing CuS. The preparation conditions of PbS were $Pb(CH_3COO)_2{\cdot}3H_2O$ (3.0 g), solvent (70.0 g), and reaction temperature (180 °C) for 24 h. The preparation conditions of ZnS were $Zn(NO_3)_2{\cdot}6H_2O$ (1.0 g), solvent (40.0 g), and reaction temperature (180 °C) for 12 h.

Preparation of electrodes

The prepared metal chalcogenides (MC, 12.0 mg) was suspended in 2 mL ethanol with 40 μL Nafion D-521 dispersion (5 wt%) to form a homogeneous ink with the assistance of ultrasound. After that, 1 mL of the ink was spread onto the carbon paper (CP) surface (1 cm×1 cm), and then was dried under room temperature. Finally, these electrodes were obtained, and denoted as MC/CP.

Characterization

A transmission electron microscopy (TEM) JEOL-1011 with an accelerating voltage of 120 kV was used for the TEM characterization. The scanning electron microscopy (SEM) experiment was conducted on a Hitachi S-4800 scanning electron microscope operated at 15 kV. Powder X-ray diffraction (XRD) patterns were collected on a Rigaku D/max-2500 X-ray diffractometer using Cu Kα radiation (λ = 0.154 nm). X-ray photoelectron spectroscopy (XPS) measurements were carried out on an ESCAL Lab 220i-XL specrometer. ^{1}H NMR spectra were recorded on a Bruker Avance III HD 400 MHz NMR spectrometer.

Linear sweep voltammetry (LSV) measurements

All the electrochemical experiments in the work were conducted using the electrochemical workstation (CHI 660E, Shanghai CH Instruments Co., China). An H-type cell separated by Nafion 117 membrane was used for the linear sweep voltammetry (LSV) measurements. There were three electrodes in the system including working electrode (MC/CP), a platinum gauze auxiliary electrode, and an Ag/Ag^+ (0.01 M $AgNO_3$ in 0.1 M TBAP-MeCN) reference electrode. Prior to experiment, the air in electrolyte was removed by bubbling with N_2 for 30 minutes. The LSV measurement was performed in the potential range of 0.3 to 1.9 V *vs.* Ag/Ag^+ at a sweep rate of 20 $mV \cdot s^{-1}$. The process was carried out under the slight magnetic stirring.

Electrochemical impedance spectroscopy (EIS)

The EIS experiment was conducted in a single compartment cell with three electrodes, namely, working electrode, a platinum gauze auxiliary electrode, and Ag/Ag^+ (0.01 M $AgNO_3$ in 0.1 M TBAP-MeCN) reference electrode. The EIS spectra were collected using potentiostatic mode at an open circuit potential of 100 kHz to 100 mHz with an amplitude of 5 mV. The EIS data were fitted by the ZSimpwin software.

Electrocatalytic oxidation of furfural and product analysis

Electrochemical oxidation of furfural was performed in a typical H-type cell at room temperature, which was similar with that used for electrochemical reduction of CO_2.[32] The anodic and cathodic electrolytes were $[Et_3NH]NO_3$-MeCN-H_2O and aqueous H_2SO_4 solution (0.2 M), respectively, and the amount of electrolyte in each chamber was 5.6 g in all experiments. Prior to electrolysis, N_2 was bubbled through the anolyte for 30 min under stirring. Then, furfural (1 mmol) was added into the anolyte, and the electrochemical reaction was started at a desired applied potential. After the reaction was conducted for suitable reaction time, the liquid product was analyzed by ^1H NMR (Bruker Avance III 400 HD spectrometer) in D_2O. The gaseous product was analyzed by gas chromatography (GC, HP 4890D) equipped with TCD detector using helium as the internal standard. The conversion and selectivity of the reaction were calculated according to NMR and GC analysis.

Conflicts of interest

There are no conflicts to declare.

Acknowledgements

This work was supported by National Natural Science Foundation of China (21673249, 21733011), the National Key Research and Development Program of China (2017YFA0403103), Key Research Program of Frontier Sciences, CAS (QYZDY-SSW-SLH013), and Youth Innovation Promotion Association of Chinese Academy of Sciences (2017043).

Notes and references

1 Y. Shao, Q. Xia, L. Dong, X. Liu, X. Han, S. F. Parker, Y. Cheng, L. L. Daemen, A. J. Ramirez-Cuesta, S. Yang and Y. Wang, *Nat. Commun.,* 2017, **8**, 16104.
2 G. Liang, A. Wang, L. Li, G. Xu, N. Yan and T. Zhang, *Angew. Chem. Int. Ed.,* 2017, **56**, 3050-3054.
3 H. Guo, D. M. Miles-Barrett, A. R. Neal, T. Zhang, C. Li and N. J. Westwood, *Chem. Sci.,* 2018, **9**, 702-711.
4 L. T. Mika, E. Cséfalvay and Á. Nemeth, *Chem. Rev.,* 2018, **118**, 505-613.
5 M. Wang, H. Shi, D. M. Camaioni and J. A. Lercher, *Angew. Chem. Int. Ed.,* 2017, **56**, 2110-2114.
6 S. Chen, R. Wojcieszak, F. Dumeignil, E. Marceau and S. Royer, *Chem. Rev*., 2018, **118**, 11023-11117.
7 D. Chandra, Y. Inoue, M. Sasase, M. Kitano, A. Bhaumik, K. Kamata, H. Hosono and M. Hara, *Chem. Sci.,* 2018, **9**, 5949-5956.
8 N. Brun, P. Hesemann and D. Esposito, *Chem. Sci.,* 2017, **8**, 4724-4738.
9 P. Kumar and R. K. Pandey, *Green Chem.,* 2000, **2**, 29-31.
10 J. Boukouvalas and N. Lachance, *Synlett,* 1998, **1**, 31-32.
11 X. Li, B. Ho, D. S. W. Lim and Y. Zhang, *Green Chem.,* 2017, **19**, 914-918.
12 Y. Rodenas, R. Mariscal, J. L. G. Fierro, D. M. Alonso, J. A. Dumesic and M. L. Granados, *Green Chem.,* 2018, **20**, 2845-2856.
13 J. M. Carney, R. J. Hammer, M. Hulce, C. M. Lomas and D. Miyashiro, *Synthesis,* **2012**, 44, 2560-2566.
14 B. M. Trost and F. D. Toste, *J. Am. Chem. Soc.,* 2003, **125**, 3090-3100.
15 Y. Morita, H. Tokuyama and T. Fukuyama, *Org. Lett.,* 2005, **7**, 4337-4340.
16 S. Barwe, J. Weidner, S. Cychy, D. M. Morales, S. Dieckhöfer, D. Hiltrop, J. Masa, M. Muhler and W. Schuhmann, *Angew. Chem. Int. Ed.,* 2018, **57**, 11460-11464.
17 X. Lu and C. Zhao, *Nat. Commun.,* 2015, **6**, 6616.
18 F. Franco, M. F. Pinto, B. Royo and J. Lloret-Fillol, *Angew. Chem. Int. Ed.,* **2018**, 57, 4603-4606.
19 Z. Ji, C. Trickett, X. Pei and O. M. Yaghi, *J. Am. Chem. Soc.,* 2018, **140**, 13618-13622.
20 X. H. Chadderdon, D. J. Chadderdon, J. E. Matthiesen, Y. Qiu, J. M. Carraher, J.-P. Tessonnier and W. Li, *J. Am. Chem. Soc.,* 2017, **139**, 14120-14128.
21 N. Jiang, B. You, R. Boonstra, I. M. T. Rodriguez and Y. Sun, *ACS Energy Lett.,* 2016, **1**, 386-390.
22 S. Cotillas, J. Llanos, P. Canizares, D. Clematis, G. Cerisola, M. A. Rodrigo and M. Panizza, *Electrochim. Acta,* 2018, **263**, 1-7.
23 B. Marselli, J. Garcia-Gomez, P.-A. Michaud, M. A. Rodrigo and C. Comninellis, *J. Electrochem. Soc.,* 2003, **150**, 79-83.
24 H. Hamad, D. Bassyouni, E. El-Ashtoukhy, N. Amin and M. A. El-Latif, *Ecotox. Environ. Safe,* 2018, **148**, 501-512.
25 A. Kapałka, G. Fóti and C. Comninellis, *Electrochimica Acta,* 2009, **54**, 2018-2023.
26 T. A. Enache, A.-M. Chiorcea-Paquim, O. Fatibello-Filho and A. M. Oliveira-Brett, *Electrochem. Commun.,* 2009, **11**, 1342-1345.
27 M. A. Q. Alfaro, S. Ferro, C. A. Martínez-Huitle and Y. M. Vong, *J. Braz, Chem. Soc.,* 2006, **17**, 227-236.
28 Y. Huang, R. J. Nielsen and W. A. Goddard, III, *J. Am. Chem. Soc.,* 2018, **140**, 16773-16782.
29 M.-R. Gao, M. K. Y. Chan and Y. Sun, *Nat. Commun.,* 2015, **6**, 7493.
30 M. Hesari, K. N. Swanick, J.-S. Lu, R. Whyte, S. Wang and Z. Ding, *J. Am. Chem. Soc.,* 2015, **137**, 11266-11269.
31 X. Hong, Z. Xu, F. Zhang, C. He, X. Gao, Q. Liu, W. Guo, X. Liu and M. Ye, *Mater. Lett.,* 2017, **203**, 73-76.
32 X. Sun, Q. Zhu, X. Kang, H. Liu, Q. Qian, Z. Zhang and B. Han, *Angew. Chem. Int. Ed.,* 2016, **55**, 6771-6775.

View Article Online
DOI: 10.1039/C9SC00322C

33 K. S. W. Sing, D. H. Everett, R. A. W. Haul, L. Moscou, R. A. Pierotti, J. Rouquérol and T. Siemieniewska, Pure Appl. Chem., 1985, 57, 603-619.
34 Y. Zhao, J. Zhang, B. Han, J. Song, J. Li and Q. Wang, Angew. Chem. Int. Ed., 2011, 50, 636-639.
35 Z. Sun, T. Ma, H. Tao, Q. Fan and B. Han, *Chem,* 2017, **3**, 560-587.
36 S. Garcia-Segura, J. D. Ocon and M. N. Chong, *Process Saf. Environ. Prot.,* 2018, **113**, 48-67.
37 J. Jiang, C. Yan, X. Zhao, H. Luo, Z. Xue and T. Mu, *Green Chem.,* 2017, **19**, 3023-3031.

View Article Online
DOI: 10.1039/C9SC00322C

Graphical abstract

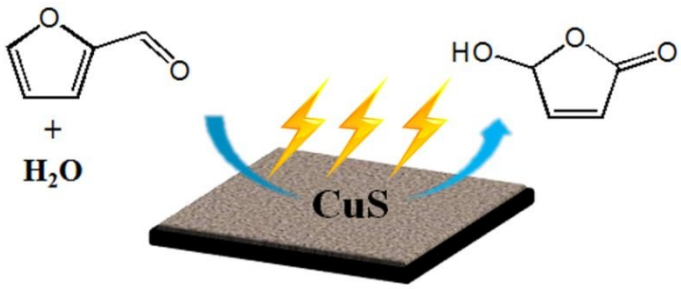

The electrocatalytic route was firstly developed for conversion of biomass-derived furfural to the bioactive 5-hydroxy-2(5H)-furanone over CuS nanosheets using H_2O as the oxygen source.